The Importance of Excluded Solvent Volume Effects in Computing Hydration Free Energies

Pei-Kun Yang[†,§] and Carmay Lim*[,†,‡]

Institute of Biomedical Sciences, Academia Sinica, Taipei 115, Taiwan R.O.C, and National Tsing Hua University, Hsinchu 300, Taiwan R.O.C

Received: March 5, 2008; Revised Manuscript Received: July 1, 2008

Continuum dielectric methods such as the Born equation have been widely used to compute the electrostatic component of the solvation free energy, ΔG_{solv}^{elec}, because they do not need to include solvent molecules explicitly and are thus far less costly compared to molecular simulations. All of these methods can be derived from Gauss Law of Maxwell's equations, which yields an analytical solution for the solvation free energy, ΔG_{Born}, when the solute is spherical. However, in Maxwell's equations, the solvent is assumed to be a structureless continuum, whereas in reality, the near-solute solvent molecules are highly structured unlike far-solute bulk solvent. Since we have recently reformulated Gauss Law of Maxwell's equations to incorporate the near-solute solvent structure by considering excluded solvent volume effects, we have used it in this work to derive an analytical solution for the hydration free energy of an ion. In contrast to continuum solvent models, which assume that the normalized induced solvent electric dipole density P_n is constant, P_n mimics that observed from simulations. The analytical formula for the ionic hydration free energy shows that the Born radius, which has been used as an adjustable parameter to fit experimental hydration free energies, is no longer ill defined but is related to the radius and polarizability of the water molecule, the hydration number, and the first peak position of the solute−solvent radial distribution function. The resulting ΔG_{solv}^{elec} values are shown to be close to the respective experimental numbers.

Introduction

The solvation free energy, ΔG_{solv}, is important for predicting the behavior of solute molecules in a condensed medium and in studying biological problems such as protein folding[1−6] and protein−ligand interactions.[7−11] Consequently, many methods have been developed for evaluating the solvation free energy, including free-energy simulations,[12−18] Monte Carlo simulations,[4,19−22] integral equations,[22−29] solvent-accessible surface area calculations,[30−35] and continuum dielectric methods.[36−40] The latter, including the Born equation,[41] the generalized Born equation,[33,42−46] and the Poisson equation,[47] have been widely used to compute the electrostatic component of the solvation free energy, ΔG_{solv}^{elec}, because they are less costly compared to simulations including explicit solvent molecules. All of these equations can be derived from Gauss Law of Maxwell's equations, that is, $\nabla \bullet \boldsymbol{D} = \rho_{free}$, where $\boldsymbol{D}$ is the electric displacement and ρ_{free} is the solute charge density.

In 1920, Born[41] derived the ΔG_{solv}^{elec} by charging up $\Phi(q)$, the electrostatic potential at a solute due to the polarized solvent molecules

$$\Delta G_{solv}^{elec} = \int_0^Q \Phi(q)\mathrm{d}q \qquad (1)$$

He estimated $\Phi(q)$ using Gauss law by considering a spherical ion of radius R_{Born} and charge Q immersed in a solvent with dielectric constant ε_r. The ion polarizes the solvent, generating an induced surface charge $q_{surface} = -q(1 - 1/\varepsilon_r)$, which makes a contribution of $-q(1 - 1/\varepsilon_r)/(4\pi\varepsilon_0 R_{Born})$ to the electrostatic potential at the ion, where ε_0 is the permittivity of free space.[48,49] Substituting the latter into eq 1, the free energy for transferring an ion from vacuum to a medium characterized by dielectric constant ε_r is given by

$$\Delta G_{Born}(\text{in kcal/mol}) = -166Q^2(1 - 1/\varepsilon_r)/R_{Born} \qquad (2)$$

The above derivation of the ΔG_{Born} shows that the key factor determining the ΔG_{solv}^{elec} is the accuracy of the induced solvent surface charge density or electric dipole density $\boldsymbol{P}$. However, the induced solvent density ρ is assumed to be uniform, equal to the bulk solvent density ρ_{bulk} in Gauss law, whereas the ρ near a charged solute may be several fold greater than ρ_{bulk} in molecular dynamics (MD) simulations.[50] Furthermore, the induced solvent charge density ρ_q multiplied by the surface area, $4\pi r^2$, for a spherical ion of charge Q derived from Gauss law differs from $4\pi r^2\rho_q$ computed from simulations (Figure 1). For an uncharged solute, the $4\pi r^2\rho_q$ is zero everywhere according to Gauss law but oscillates by as large as ±2.5 e/Å during the simulation. For a charged solute, the $4\pi r^2\rho_q$ predicted from Gauss law is the surface charge density at the solute−solvent interface, but it decays in an oscillatory manner from the solute in simulations. As the induced solvent charge density differs for solutes of different charges but the same van der Waals (vdW) parameters, a simple equation linking ρ_q to Q is not straightforward.

Consequently, to reproduce the experimental hydration free energies, ΔG_{hydr}^{expt}, the Born radius R_{Born}, which was arbitrarily defined in deriving eq 2, has been used as a parameter to fit the

* To whom correspondence should be addressed. E-mail: carmay@gate.sinica.edu.tw.
† Academia Sinica.
‡ National Tsing Hua University.
§ Department of Biomedical Engineering, I-Shou University, Kaohsiung 840, Taiwan, R.O.C.

10.1021/jp801960p CCC: $40.75
Published on Web 10/29/2008

ΔG_{hydr}^{expt}. For a solute composed of n atoms, there are n Born radii parameters but only one ΔG_{hydr}^{expt}; hence, numerous sets of Born radii can be adjusted to fit the ΔG_{hydr}^{expt}. For example, a set of atomic Born radii defining the dielectric boundary between the solute and the solvent in continuum electrostatic models has been obtained initially from an analysis of the induced solvent charge distribution function and subsequently refined to reproduce the ΔG_{solv}^{elec} from free-energy simulations.[51] The ΔG_{hydr}^{expt} can be expressed as an integration of the solute hydration free energy weighted by the probability of finding the solute in a given conformation over all possible solute conformations. The probability of finding the solute in a given conformation depends on its environment. For example, the probability of finding solute A well separated from solute B differs from that of finding solute A covalently bonded to B. Thus, the n Born radii parameters do not suffice to fit the ΔG_{hydr}^{expt} derived from numerous solute conformations unless the function that describes the ΔG_{hydr}^{expt} for various solute conformations is accurate enough. Although methods such as computer simulations and quantum mechanics can yield an accurate hydration free energy for a solute molecule, how ΔG_{hydr} changes as the solute conformation changes cannot be guessed or estimated before numerical calculations have been performed. In contrast, an analytical solution such as eq 2 can provide insight as to how the ΔG_{hydr}^{elec} for different charged ions changes.

Herein, we address the following questions: First, since the Born equation, which is based on Gauss law, does not account for the near-solute solvent structure, is it possible to find an analytical solution for the induced solvent $\boldsymbol{P}$ for a spherical ion immersed in a solvent of dielectric constant ε_r that can mimic $\boldsymbol{P}$ from MD simulations? Second, is it possible to relate the Born radius, R_{Born}, to some physical observable rather than treating it as an adjustable parameter? To address these questions, we derive herein an analytical solution for the ΔG_{hydr}^{elec} of a monatomic solute from "microscopic" Gauss law, which has recently been formulated to take into account the near-solute solvent structure.[50,52] Like macroscopic Gauss law, $\nabla \cdot \boldsymbol{D} = \rho_{free}$, but unlike macroscopic Gauss Law where $\boldsymbol{D} = \varepsilon_0 \boldsymbol{E} + \boldsymbol{P}$, it is related to the electric field $\boldsymbol{E}$ acting on the solvent molecule at $\boldsymbol{r}$ in "microscopic" Gauss Law by

$$\boldsymbol{D}(\boldsymbol{r}) = \varepsilon_0 \boldsymbol{E}(\boldsymbol{r}) - \int [\nabla' \cdot \boldsymbol{P}'(\boldsymbol{r}';\boldsymbol{r})] \nabla(1/4\pi R) \mathrm{d}^3 \boldsymbol{r}' \quad (3)$$

The second term in eq 3 denotes the contribution to $\boldsymbol{D}$ from the perturbed solvent dipole density $\boldsymbol{P}'(\boldsymbol{r}';\boldsymbol{r})$ due to the solvent dipole at $\boldsymbol{r}$. Notably, the numerical solution from "microscopic" Gauss law can reproduce the oscillatory decay of the relative water density ρ/ρ_{bulk} and the induced solvent $\boldsymbol{P}$ observed from MD simulations simply by considering excluded solvent volume effects, that is, each water molecule occupies volume, thus excluding other water molecules.[52] Below, we first compute the induced solvent $\boldsymbol{P}$ from MD simulations of a solute atom of varying charge Q (−1, 0, and +1 e) in TIP3P water.[53] We then propose a simple functional form for the induced solvent $\boldsymbol{P}$ mimicking that from MD simulations. The approximate induced solvent $\boldsymbol{P}$ was used to yield an analytical solution to $\Phi(q)$ and thus ΔG_{hydr}^{elec} from eq 1.

Methods

MD Simulations of a Solute Atom in TIP3P Water. The MD simulations were carried out in an NVE ensemble using the CHARMM program[54] and spherical boundary conditions without cutoffs.[55,56] The ion−water and water−water interaction energies were modeled by a sum of Coulomb and van der Waals (vdW) pairwise energies. For the solute atom, the charges are −1, 0, and +1 e, and the vdW parameters were assigned to be those of the TIP3P water oxygen with $\varepsilon = -0.1521$ kcal/mol and $R_{min}/2 = 1.7682$ Å. For TIP3P water, the oxygen and hydrogen atomic charges are −0.834 and +0.417 e, respectively, while the hydrogen vdW parameters are $\varepsilon = -0.046$ kcal/mol and $R_{min}/2 = 0.2245$ Å. The TIP3P O−H bond length, 0.9572 Å, and the H−O−H bond angle, 104.52°, were constrained during the simulations using the SHAKE algorithm.[57]

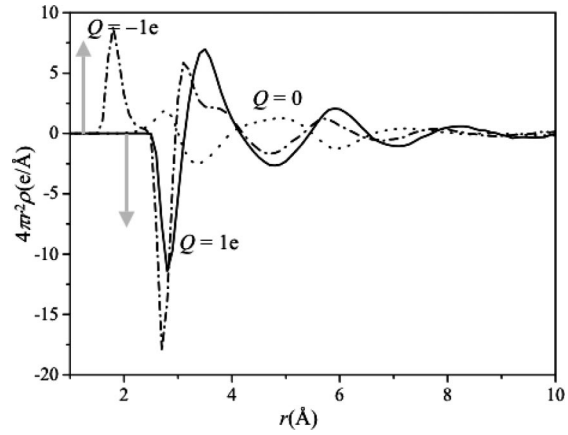

Figure 1. Comparison of the induced solvent charge density derived from MD simulations and macroscopic Gauss law. The induced solvent charge density multiplied by the surface area, $4\pi r^2\rho$, as a function of the distance r from the solute was derived from MD simulations of an atom of charge −1 (dashed curves), 0 (dotted curves), and +1e (solid curves) solvated with explicit water molecules as well as from macroscopic Gauss law (gray arrows).

The solute atom was fixed at the center of a 15 Å radius sphere containing previously equilibrated water molecules at an experimental density of 0.0334 molecules/Å^3. The water molecule that overlapped with the solute atom was removed, resulting in 471 water molecules. All atoms were propagated according to Newton's equations using the leapfrog Verlet algorithm and a time step of 2 fs at a mean temperature of 300 K. Each system was first minimized for 1000 steps and equilibrated for 100 ps. It was then subjected to 4 ns of production dynamics, and configurations were stored every 20 fs to compute the induced $\boldsymbol{P}$.

Computing the Water Charge Density ρ_q and Electric Dipole Density P_a. From the stored configurations in the MD trajectory, ρ_q was obtained by counting the net charge in the annular space between $(r - \Delta r)$ and $(r + \Delta r)$ during the simulation

$$\rho_q(r) = \frac{1}{4\pi r^2 dr N_c} \int_{r-\Delta r/2}^{r+\Delta r/2} \sum_{l=1}^{N_c} \sum_{m=1}^{n} \sum_{i=1}^{3} q_i \delta(r - r_i^{lm}) \mathrm{d}r \quad (4)$$

In eq 4, the first summation is over the N_c stored configurations,[50] the second summation is over the n water molecules in the simulation system, the third summation is over the three water atoms, q_i is the water oxygen/hydrogen charge, r is the distance from the solute atom, and r_i^{lm} denotes the distance of the ith atom of water molecule m in configuration l from the solute. The induced $\boldsymbol{P}$ was computed by counting the average dipole moment of those water molecules whose oxygen r_o^{lm} positions are between $(r - \Delta r)$ and $(r + \Delta r)$ during the simulation

$$\boldsymbol{P}(r) = \frac{1}{4\pi r^2 \mathrm{d}r N_c} \int_{r-\Delta r/2}^{r+\Delta r/2} \sum_{l=1}^{N_c} \sum_{m=1}^{n} \sum_{i=1}^{3} q_i r_i^{lm} \delta(r - r_o^{lm}) \mathrm{d}r \tag{5}$$

Results

Including the near-Solute Water Structure Observed in MD Simulations in the *P*. To obtain a simple functional form for the induced ***P*** that could yield an analytical solution for the hydration free energy of an ion, we first examined how the normalized induced water electric dipole density, $P_n = 4\pi r^2 P/Q$, obtained from MD simulations behaves as a function of the distance from the solute atom, r. Whereas P_n from macroscopic Gauss law is a constant equal to $1 - 1/\varepsilon_r$, it decays in an oscillatory manner to unity with increasing r (Figure 2). The P_n exhibits a large peak at around $r = r_{max}$, which differs depending on the solute charge, and a much smaller peak at around ~5.4 Å; after the second hydration shell, it roughly plateaus. Note that r_{max} is close to but not identical to the first peak position of the solute−O radial distribution function, R_{gmax}.[50] Because the valley between the first and second peak of P_n is almost zero, P_n was decomposed into contributions from the structured first-shell water molecules and water molecules beyond the first hydration shell. The latter were treated as bulk water; hence, for r greater than the sum of R_{gmax} and R_w, the radius of the water molecule, P_n was approximated by $1 - 1/\varepsilon_r$, as in macroscopic Gauss law. At r_{max}, P_n is at its maximum and was approximated by $P_s(R_{gmax})$, the surface dipole density at R_{gmax} rather than that at r_{max} as R_{gmax} can be experimentally measured (see below).

The Surface Dipole Density at R_{gmax}. To compute $P_s(R_{gmax})$, consider a water molecule, which was treated as a perfect dipole at the center of a hard sphere, located at a distance of $z = R_{gmax}$ from a solute atom of charge Q (Figure 3). The electric potential at this water molecule, $\Phi(R_{gmax})$, comprises contributions from the solute and water molecules polarized by both the solute and the water molecule at R_{gmax}. As a first approximation, polarization effects from the water molecule at R_{gmax} were neglected.

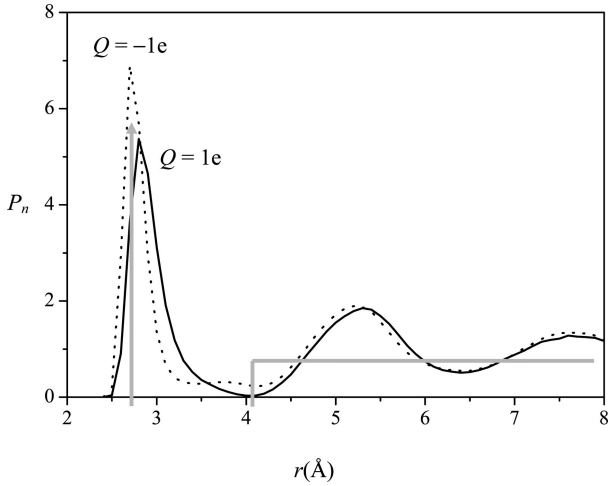

Figure 2. Approximating the normalized induced solvent dipole density derived from MD simulations. For an atom of charge −1 (dotted curves) or +1 e (solid curves), the normalized induced solvent dipole density P_n as a function of the distance r from the solute was derived from MD simulations of an atom of charge −1 (dashed curves) and +1 e (solid curves) solvated with explicit water molecules. It was approximated by $P_s(R_{gmax})$, the surface dipole density at R_{gmax} (gray arrow) and a constant equal to $1 - 1/\varepsilon_r$ for r greater than the sum of R_{gmax} and R_w.

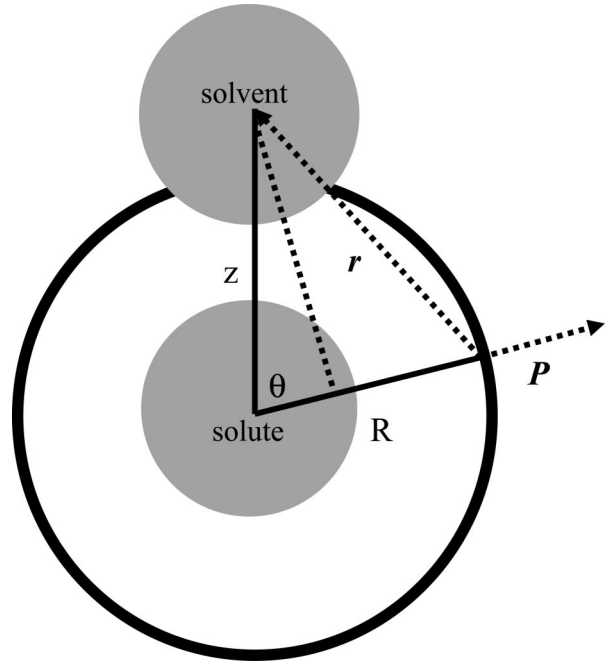

Figure 3. Schematic diagram showing the derivation of the surface dipole density at R_{gmax}. A water molecule (gray solvent) is located at a distance z from a solute atom of charge Q at the origin; r is the distance between the fixed solvent molecule at z and the solvent dipole density at a distance R from the solute and at an angle θ from the z-axis.

In general, the contribution to the electric potential at a distance z from water dipoles in the annular space between R and $R + \mathrm{d}R$ is given by (see the Appendix)

$$\Phi'(z) = 2\pi R^2 \mathrm{d}R \int_{\theta_w}^{\pi} \mathrm{d}\Phi(R) \sin\theta \, \mathrm{d}\theta = \frac{P(R)\mathrm{d}R}{2\varepsilon_0}\left(\frac{z^2 - R^2 + R_W^2}{2zR_W} - 1\right) \tag{6}$$

where $P(R)$ is the water dipole density at a distance R from the solute atom and R_w is the radius of the water molecule, $R_W = (z^2 + R^2 - 2zR\cos\theta_W)^{1/2}$. The corresponding electric field at a distance z from the solute atom, $E'(z)$, is

$$E'(z) = -\frac{\mathrm{d}\Phi'(z)}{\mathrm{d}z} = -\frac{P(R)\mathrm{d}R}{4\varepsilon_0}\frac{z^2 + R^2 - R_W^2}{z^2 R_W} \tag{7}$$

Because the water dipole density is spherically symmetrical for $R < z - R_w$ and $R > z + R_w$, it makes no contribution to the electric field. Hence, only water molecules in the annular space between $z - R_w$ and $z + R_w$ and the solute contribute to the electric field along z direction, that is

$$E(z) = -\frac{1}{4\varepsilon_0 R_W z^2}\int_{z-R_W}^{z+R_W} P(R)(z^2 + R^2 - R_W^2)\mathrm{d}R + \frac{Q}{4\pi\varepsilon_0 z^2} \tag{8a}$$

Equation 8a can be rearranged in the form of the "microscopic" dielectric displacement ***D*** (eq 3), where $\mathbf{D} = Q/4\pi z^2$ and $-\int \nabla' \cdot \mathbf{P}'(\mathbf{r}';\mathbf{r}))\nabla(1/4\pi R)\mathrm{d}^3\mathbf{r}' = 1/(4R_W z^2)\int_{z-R_W}^{z+R_W} P(R)(z^2 + R^2 - R_W^2)\mathrm{d}R$. Since the water dipole density in the region of $R_{gmax} -$

R_W to $R_{gmax} + R_W$ is assumed to be equal to $P_s\delta(R - R_{gmax})$ (see above and Figure 2), substituting $z = R_{gmax}$ in eq 8a yields

$$E(R_{gmax}) = -\frac{1}{4\varepsilon_0 R_W R_{gmax}^2} P_s(R_{gmax})(2R_{gmax}^2 - R_W^2) + \frac{Q}{4\pi\varepsilon_0 R_{gmax}^2} \quad (8b)$$

Equation 8b can be rewritten to show how $E(R_{gmax})$ and $P_s(R_{gmax})$ are related to the solute charge

$$4\pi\varepsilon_0 R_{gmax}^2 E(R_{gmax}) + \frac{\pi}{R_W} P_s(R_{gmax})(2R_{gmax}^2 - R_W^2) = Q \quad (8c)$$

The surface dipole density P_s can be decomposed into the product of the number of water molecules per surface area σ and the dipole moment per water molecule p that is, $P_s(R_{gmax}) = \sigma p(R_{gmax})$. The $p(R_{gmax})$ is proportional to the electric field E acting on the water molecule at R_{gmax}, that is, $p(R_{gmax}) = \varepsilon_0\gamma_e E(R_{gmax})$, where γ_e is the molecular polarizability of water. Hence, $P_s(R_{gmax}) = \sigma\varepsilon_0\gamma_e E(R_{gmax})$. Substituting $E(R_{gmax}) = P_s(R_{gmax})/\sigma\varepsilon_0\gamma_e$ into eq 8c yields

$$P_s(R_{gmax}) = \frac{CQ}{4\pi R_{gmax}^2} \quad (9)$$

where C is given by

$$C = 1\Big/\left(\frac{1}{2R_W} - \frac{R_W}{4R_{gmax}^2} + \frac{1}{\gamma_e\sigma}\right) \quad (10)$$

Deriving the Hydration Free Energy from the Water Dipole Density. To derive an analytical formula for the hydration free energy, we first decomposed the electrostatic potential at the solute, $\Phi(q)$, into contributions from (i) the first-shell water molecules, $\Phi_1(q)$, and (ii) water molecules beyond the first shell, $\Phi_{bulk}(q)$. For $R \le R_{gmax}$, the surface dipole density at R, $P_s(R_{gmax})$, or the net outward dipole moment at R, $4\pi R_{gmax}^2 P_s(R_{gmax})$, contribute

$$\Phi_1(q) = -\frac{4\pi R_{gmax}^2 P_s(R_{gmax})}{4\pi\varepsilon_0 R_{gmax}^2} = -\frac{P_s(R_{gmax})}{\varepsilon_0} = -\frac{Cq}{4\pi\varepsilon_0 R_{gmax}^2} \quad (11a)$$

For $R > R_{gmax} + R_W$, the water molecules are treated like bulk water, and therefore, the net induced surface charge in the shell at a distance of $R_{gmax} + R_W$ from the solute is $-q(1 - 1/\varepsilon_r)$; hence

$$\Phi_{bulk}(q) = -\frac{1}{4\pi\varepsilon_0}\frac{(1 - 1/\varepsilon_r)q}{R_{gmax} + R_W} \quad (11b)$$

Substituting eqs 11a and 11b into eq 1, the ΔG_{hydr}^{elec} is given by

$$\Delta G_{hydr}^{elec} = \int_0^Q [\Phi_1(q) + \Phi_{bulk}(q)]dq = -166Q^2\left[\frac{C}{R_{gmax}^2} + \frac{(1 - 1/\varepsilon_r)}{R_{gmax} + R_W}\right] \quad (12)$$

Comparing eq 12 with eq 2 yields

$$\frac{(1 - 1/\varepsilon_r)}{R_{Born}} = \frac{C}{R_{gmax}^2} + \frac{(1 - 1/\varepsilon_r)}{R_{gmax} + R_W} \quad (13a)$$

$$R_{Born} = \frac{R_{gmax}^2(R_{gmax} + R_W)}{R_{gmax}^2 + C(R_{gmax} + R_W)} \quad (13b)$$

The Born radius is no longer arbitrarily defined but is related to the R_{gmax}, R_W, σ, and γ_e by eq 13.

Comparing the Computed and Experimental Hydration Free Energies. To assess the accuracy of eq 12, the ΔG_{hydr}^{elec} of ions of charge Q varying from -1 to $+3$ were computed from eq 12 and compared with the respective experimental numbers (see Table 1). Computing ΔG_{hydr}^{elec} requires knowledge of R_{gmax}, R_W, σ, and γ_e. The R_{gmax} values for the ions listed in Table 1 have been measured,[58] and their experimental values are listed in Table 1. The water radius R_W of 1.4 Å was assumed to be equal to half of the R_{gmax} of the O−O distribution function of liquid water at 25 °C obtained from neutron diffraction.[59] Knowing R_{gmax}, the water surface density at R_{gmax}, $\sigma(R_{gmax})$, was computed by dividing the first-shell coordination number of the ion, which gives the number of water molecules at R_{gmax}, by the surface area $4\pi R_{gmax}^2$. The γ_e of water (46.4) was obtained from the ratio of the average water dipole moment $\boldsymbol{p}$ to the applied field $\boldsymbol{E}$ at the water molecule using Langevin's equation, as described in our previous work.[52]

The results show that the ΔG_{hydr}^{elec} computed from eq 12 are generally close to the respective experimental ΔG_{hydr}^{elec}. Among the 29 ions in Table 1, the predicted ΔG_{hydr}^{elec} values of 22 ions are within 10% of the respective experimental values. These percentage errors seem reasonable considering that (a) the experimental ΔG_{hydr}^{expt} obtained using different methods may differ by as large as 5% difference (e.g., Cr^{3+})[60] and (b) the ΔG_{hydr}^{expt} includes not only ΔG_{hydr}^{elec} but also the free energy to form the cavity in aqueous solution, which has been neglected in this work. The other ions differ from the experimental numbers by 10−20% (see Discussion). The first hydration shell contributes 46, 52, 57, and 60% of the net ΔG_{hydr}^{elec} for an ion of charge −1, +1, +2, and +3, respectively. This indicates that the contribution of the first hydration shell to the net ΔG_{hydr}^{elec} depends not only on the magnitude of the solute charge but also on its sign.

Discussion

A proper description of the induced solvent $\boldsymbol{P}$ is needed to compute the Φ at the solute and thus the G_{solv}^{elec}. This work proposes a functional form for the induced solvent $\boldsymbol{P}$ that is more accurate than that in continuum solvent models (see below and Figure 2). Only water molecules outside of the first hydration shell ($R > R_{gmax} + R_W$,) are treated like bulk water with the normalized $P_n = 1 - 1/\varepsilon_r$; however, those in the first shell ($R \le R_{gmax}$) are assumed to yield an induced surface electric dipole density at R_{gmax}, whose amplitude was solved by considering excluded volume effects (eq 9). With these approximations to P_n, analytical solutions for $\Phi(q)$ in the near-

TABLE 1: Comparison between the Computed and Experimental ΔG_{hydr}^{elec}

ion	Q	R_{gmax}[a]	$-\Delta G_{exp}$[b]	$-\Delta G_{cal}$[c]	%error[d]	ion	Q	R_{gmax}[a]	$-\Delta G_{exp}$[b]	$-\Delta G_{cal}$[c]	%error[d]
F	−1	2.63	103.8	85.6	−17.5	Mn	2	2.19	437.8	441.1	0.7
Cl	−1	3.19	75.8	66.3	−12.5	Fe	2	2.11	456.4	465.1	1.9
Br	−1	3.37	72.5	61.8	−14.7	Co	2	2.11	479.5	465.1	−3.0
I	−1	3.65	61.4	55.9	−8.9	Ni	2	2.06	494.2	481.4	−2.6
Li	1	2.08	123.5	118.7	−3.9	Cu	2	2.11	498.7	465.1	−6.7
Na	1	2.36	98.3	99.3	1.0	Zn	2	2.10	484.6	468.3	−3.4
K	1	2.80	80.8	78.7	−2.6	Cd	2	2.30	430.5	411.7	−4.4
Rb	1	2.89	76.6	75.5	−1.5	Hg	2	2.42	436.3	383.6	−12.1
Cs	1	3.14	71	67.7	−4.6	Sn	2	2.33	371.4	404.3	8.9
Ag	1	2.42	114.5	95.9	−16.2	Al	3	1.89	1103.3	1227.8	11.3
Be	2	1.75	582.3	611.9	5.1	Cr	3	1.97	1037	1155.5	11.4
Mg	2	2.09	455.5	471.5	3.5	Fe	3	2.03	1035.5	1106.3	6.8
Ca	2	2.42	380.8	383.6	0.7	In	3	2.16	973.2	1012.1	4.0
Sr	2	2.64	345.9	340.6	−1.5	Tl	3	2.23	975.9	967.4	−0.9
Ba	2	2.90	315.1	300.5	−4.6						

[a] Values from Marcus, 1988.[58] [b] Values from Friedman, 1973.[68] [c] ΔG_{cal} computed from eq 12 using $C = 1.85$. [d] %error $= (\Delta G_{cal} - \Delta G_{exp})/\Delta G_{exp} \times 100$.

and far-solute regions were obtained (eq 11) and used in eq 1 to obtain an analytical solution for the ΔG_{hydr}^{elec} (eq 12). The latter shows that the ΔG_{hydr}^{elec} depends quadratically on the solute charge, Q, like ΔG_{Born}, but the radius is no longer arbitrary, unlike the Born radius, R_{Born}, in eq 2. It also shows that R_{Born} is related to R_{gmax}, the ion's hydration number, and the water radius and molecular polarizability.

Comparison with Previous Works. In contrast to the aforementioned functional form for P_n, the P_n based on macroscopic Gauss law is constant, equal to $1 - 1/\varepsilon_r$ in deriving the ΔG_{Born}, and water molecules near and far from the solute are treated in the same way as bulk water, characterized by ε_r. Adjusting the Born radius to reproduce the experimental hydration free energy is equivalent to shifting the position of the induced surface charge density, but it cannot mimic the oscillatory decay of the surface charge density from a charged solute in MD simulations (see Introduction). In contrast, the simple functional form for P_n in Figure 2 mimics that from MD simulations but does not have the disadvantage of simulations where fluctuational quantities do not easily converge. It also allows a formal derivation of R_{Born} (eq 13b), whereas in previous works (see ref 60 and references therein), R_{Born} has been empirically related to R_{gmax} and/or the ionic radius.

Comparison with Experiment. Although for most ions the ΔG_{hydr}^{elec} values predicted from eq 12 are within 10% of the respective experimental values, for some ions, the computed ΔG_{hydr}^{elec} values deviate from the respective ΔG_{hydr}^{expt} by 10−20%. This may stem from one or more of the following reasons. First, approximations were made to describe the water electric dipole density (see above and Figure 2). Second, the water molecule was treated as a perfect electric dipole moment occupying a sphere of radius R_W, but the electric effect stemming from a perfect dipole moment differs from real water molecules. Third, the electric field at R_{gmax} (eq 8b) was estimated by approximating the perturbed water effect by the water cavity. Fourth, although the first peak position of the P_n distribution in Figure 2 is located at r_{max}, the induced electric dipole surface density is assumed to be located at R_{gmax}, which is slightly different from r_{max}.

Future Work. From the above discussion, future efforts may be directed to alleviate the aforementioned limitations so as to obtain a more accurate induced water polarization and thus hydration free energy. For a multiatom solute, it would be very difficult to derive an approximate analytical solution of $\boldsymbol{P}$ and thus ΔG_{hydr}^{elec} (eq 12) based on microscopic Gauss's law, as described herein for a monatomic solute (eqs 9 and 12); hence, $\boldsymbol{P}$ needs to be solved at R_{gmax} and beyond $R_{gmax} + R_W$ using numerical methods such as boundary element techniques.[61−67] The R_{gmax} can be determined for each atom type of a multiatom solute by carrying out MD simulations of each atom type in explicit water using the assigned vdW parameters and partial charges from a given force field. The numerical solution for $\boldsymbol{P}$ can then be used to compute the ΔG_{hydr}^{elec} for a multiatom solute.

In conclusion, this work shows how an analytical solution for the solvent $\boldsymbol{P}$ and thus ion hydration free energy can be derived from microscopic Gauss law, which, unlike macroscopic Gauss law, incorporates the near-solute water structure by considering excluded solvent volume effects. Whereas the Born radius based on macroscopic Gauss law has been considered as an empirical parameter to take into account the microscopic solvent structure, the Born radius based on microscopic Gauss law is no longer adjustable but is derived from properties of both solute and solvent via eq 13.

Acknowledgment. We thank Professor Martin Karplus for the CHARMM program. This work was supported by the Institute of Biomedical Sciences, Academia Sinica, and the National Science Council, Taiwan.

Appendix

Derivation of Equation 6. The electrostatic potential at z, $d\Phi'(z)$, stemming from the solvent dipole density at a distance R from the solute, $\boldsymbol{P}(R)$, can be computed from

$$d\Phi'(z) = \frac{\boldsymbol{P}(R)\bullet\boldsymbol{r}}{4\pi\varepsilon_0 r^3}d\tau = \frac{P(R)}{4\pi\varepsilon_0}\frac{z\cos\theta - R}{(R^2 + z^2 - 2Rz\cos\theta)^{3/2}}d\tau$$

where $\cos\theta = (z^2 + R^2 - r^2)/2zR$. When r is equal to the radius of the water molecule, R_W, $\theta = \theta_W$. The contribution to the electric potential at a distance z from the solute atom from water dipoles in the annular space between R and $R + dR$ is obtained by integrating $d\Phi'(z)$ over the entire surface region as follows

$$\Phi'(z) = 2\pi R^2 \mathrm{d}R \int_{\theta_W}^{\pi} \mathrm{d}\Phi' \sin\theta \, \mathrm{d}\theta$$

$$= 2\pi R^2 \frac{P(R)\mathrm{d}R}{4\pi\varepsilon_0} \int_{\theta_W}^{\pi} \frac{z\cos\theta - R}{(R^2 + z^2 - 2Rz\cos\theta)^{3/2}} \sin\theta \, \mathrm{d}\theta$$

Let $x = \cos\theta$; then, $\mathrm{d}x = -\sin\theta \mathrm{d}\theta$

$$\Phi'(z) = \frac{R^2 P(R)\mathrm{d}R}{2\varepsilon_0} \int_{-1}^{(z^2+R^2-R_W^2)/2zR} \frac{zx - R}{(R^2 + z^2 - 2Rzx)^{3/2}} \mathrm{d}x$$

$$= \frac{RP(R)\mathrm{d}R}{2z\varepsilon_0} \int (zx - R)\mathrm{d}(R^2 + z^2 - 2Rzx)^{-1/2}$$

$$= \frac{RP(R)\mathrm{d}R}{2z\varepsilon_0} [(zx - R)(R^2 + z^2 - 2Rzx)^{-1/2} - z \times \int_{-1}^{(z^2+R^2-R_W^2)/2zR} (R^2 + z^2 - 2Rzx)^{-1/2} \mathrm{d}x]$$

$$= \frac{RP(R)\mathrm{d}R}{2z\varepsilon_0} \left(\frac{z^2 - R^2 - R_W^2}{2RR_W} + \frac{R_W - z}{R} \right)$$

$$= \frac{P(R)\mathrm{d}R}{2\varepsilon_0} \left(\frac{z^2 - R^2 + R_W^2}{2zR_W} - 1 \right)$$

References and Notes

(1) Sorenson, J. M.; Hura, G.; Soper, A. K.; Pertsemlidis, A.; Head-Gordon, T. *J. Phys. Chem. B* **1999**, *103*, 5413–5426.
(2) Zhou, R. *Proteins: Struct., Funct., Bioinf.* **2003**, *53*, 148–161.
(3) Lazaridis, T.; Karplus, M. *Biophys. Chem.* **2003**, *100*, 367–395.
(4) Kentsis, A.; Mezei, M.; Osman, R. *Biophys. J.* **2003**, *84*, 805–815.
(5) Wen, E. Z.; Hsieh, M.-J.; Kollman, P. A.; Luo, R. *J. Mol. Graphics Modell.* **2004**, *22*, 415–424.
(6) Dudev, T.; Lim, C. *J. Am. Chem. Soc.* **2007**, *129*, 12497–12504.
(7) Jackson, R. M.; Sternberg, M. J. E. *J. Mol. Biol.* **1995**, *250*, 258–275.
(8) Sheinerman, F. B.; Norel, R.; Honig, B. *Curr. Opin. Struct. Biol.* **2000**, *10*, 153–159.
(9) Noskov, S.; Lim, C. *Biophys. J.* **2001**, *81*, 737–750.
(10) Jiang, L.; Gao, Y.; Mao, F.; Liu, Z.; Lai, L. *Proteins: Struct., Funct., Genet.* **2002**, *46*, 190–196.
(11) Dudev, T.; Lim, C. *Annu. Rev. Biophys.* **2008**, *37*, 97–116.
(12) Beveridge, D. L.; DiCapua, F. M. *Free Energy via Molecular Simulation: A Primer*; ESCOM: Leiden, The Netherlands, 1989.
(13) Jayaram, B.; Fine, R.; Sharp, K.; Honig, B. *J. Phys. Chem.* **1989**, *93*, 4320–4327.
(14) Kollman, P. A. *Chem. Rev.* **1993**, *93*, 2395–2417.
(15) Jayaram, B. *J. Phys. Chem.* **1994**, *98*, 5773–5777.
(16) Straatsma, T. P. Free Energy by Molecular Simulation. In *Reviews in Computational Chemistry*; Lipkowitz, K. B.; Boyd, D. B., Eds.; VCH Publishers Inc: New York, 1996; Vol. 81, pp 1−127.
(17) Hummer, G.; Pratt, L. R.; Garcia, A. E. *J. Phys. Chem.* **1996**, *100*, 1206–1215.
(18) Radmer, R. J.; Kollman, P. A. *J. Comput. Chem.* **1997**, *18*, 902–919.
(19) Curro, J. G. *Macromolecules* **1979**, *12*,463–466.
(20) Ciccotti, G.; Frenkel, D.; McDonald, I. R. Simulation of Liquids and Solids. *Molecular Dynamics and Monte Carlo Methods in Statistical Mechanics*. Elsevier Science: Amsterdam, 1987.
(21) Jorgensen, W. L.; Tirado-Rives, J. Free Energies of Hydration for Organic Molecules from Monte Carlo Simulations. In *Perspectives in Drug Discovery and Design*; Muller, K., Ed.; ESCOM: Leiden, The Netherlands, 1995; Vol. 3, pp 123−138.
(22) Sung, B. J.; Yethiraj, A. *J. Chem. Phys.* **2003**, *119*, 6916–6924.
(23) Hansen, J. P.; McDonald, I. R. *Theory of Simple Liquids*; Academic Press: New York, 1986.
(24) Egelstaff, P. A. *An Introduction to the Liquid State*; Oxford University Press: New York, 1994.
(25) Taylor, M. P.; Lipson, J. E. G. *J. Chem. Phys.* **1998**, *109*, 7583–7590.
(26) Ten-no, S.; Iwata, S. *J. Chem. Phys.* **1999**, *111*, 4865–4868.
(27) Lombardero, M.; Martin, C.; Jorge, S.; Lado, F.; Lomba, E. *J. Chem. Phys.* **1999**, *110*, 1148–1153.
(28) Du, Q.; Beglov, D.; Roux, B. *J. Phys. Chem. B* **2000**, *104*, 796–805.
(29) Lotfollahi, M. N.; Modarress, H. *J. Chem. Phys.* **2002**, *116*, 2487–2492.
(30) Connolly, M. L. *Science* **1983a**, *221*, 709–713.
(31) Mehler, E. L.; Eichele, G. *Biochemistry* **1984**, *23*, 3887–3891.
(32) Weiser, J.; Shenkin, P. S.; Still, W. C. *J. Comput. Chem.* **1999**, *20*, 688–703.
(33) Zhu, J.; Shi, Y.; Liu, H. *J. Phys. Chem. B* **2002**, *106*, 4844–4853.
(34) Thompson, J. D.; Cramer, C. J.; Truhlar, D. G. *J. Phys. Chem. A* **2004**, *108*, 6532–6542.
(35) Stultz, C. M. *J. Phys. Chem. B* **2004**, *108*, 16525–16532.
(36) Pomelli, C. S.; Tomasi, J. *J. Comput. Chem.* **1998**, *19*, 1758–1776.
(37) Yang, P.-K.; Liaw, S.-H.; Lim, C. *J. Phys. Chem. B* **2002**, *106*, 2973–2982.
(38) Yang, P.-K.; Lim, C. *J. Phys. Chem. B* **2002**, *106*, 12093–12096.
(39) Tomasi, J. *Theor. Chem. Acc.* **2004**, *112*, 184–203.
(40) Tomasi, J.; Mennucci, B.; Cammi, R. *Chem. Rev.* **2005**, *105*, 2999–3093.
(41) Born, M. *Z. Phys.* **1920**, *1*, 45–48.
(42) Lee, M. S.; Salsbury, F. R., Jr.; Brooks, C. L., III. *J. Chem. Phys.* **2002**, *116*, 10606–10614.
(43) Onufriev, A.; Case, D. A.; Bashford, D. *J. Comput. Chem.* **2002**, *23*, 1297–1304.
(44) Im, W.; Lee, M. S.; Brooks, C. L., III. *J. Comput. Chem.* **2003**, *24*, 1691–1702.
(45) Feig, M.; Im, W.; Brooks, C. L. *J. Chem. Phys.* **2004**, *120*, 903–911.
(46) Ishizuka, T.; Terada, T.; Nakamura, S.; Shimizu, K. *Chem. Phys. Lett.* **2004**, *393*, 546–551.
(47) Feig, M.; Onufriev, A.; S., L. M.; Im, W.; Case, D.; Brooks, C. L. *J. Comput. Chem.* **2004**, *25*, 265–284.
(48) Jackson, J. D. *Classical Electrodynamics*, 3rd ed.; John Wiley & Sons: New York, 1999.
(49) Griffiths, D. J. *Introduction to Electrodynamics*, 3rd ed.; Prentice-Hall: Upper Saddle River, NJ, 1999.
(50) Yang, P.-K.; Lim, C. *J. Comput. Chem.* **2008**, doi:10.1002/jcc.21089.
(51) Nina, M.; Beglov, D.; Roux, B. *J. Phys. Chem. B* **1997**, *101*, 5239–5248.
(52) Yang, P.-K.; Lim, C. **2008**, *J. Phys. Chem. B* **2008**. *112*, 10791–10794.
(53) Jorgensen, W. L.; Chandrasekhar, J.; Madura, J. D.; Impey, R. W.; Klein, M. L. *J. Chem. Phys.* **1983**, *79*, 926–935.
(54) Brooks, B. R.; Bruccoleri, R. E.; Olafson, B. D.; States, D. J.; Swaminathan, S.; Karplus, M. *J. Comput. Chem.* **1983**, *4*, 187–217.
(55) Berkowitz, M.; McCammon, J. A. *Chem. Phys. Lett.* **1982**, *90*, 215–217.
(56) Brooks, C. L., III.; Karplus, M. *J. Chem. Phys.* **1983**, *79*, 6312–6325.
(57) Ryckaert, J. P.; Ciccotti, G.; Berendsen, H. J. C. *J. Comput. Phys.* **1977**, *23*, 327.
(58) Marcus, Y. *Chem. Rev.* **1988**, *88*, 1475–1498.
(59) Narten, A. H.; Thiessen, W. E.; Blum, L. *Science* **1982**, *217*, 1033–1034.
(60) Babu, C. S.; Lim, C. *J. Phys. Chem. B* **1999**, *103*, 7958–7968.
(61) Vorobjev, Y. N.; Grant, J. A.; Scheraga, H. A. *J. Am. Chem. Soc.* **1992**, *114*, 3189–3196.
(62) Zauhar, R. J.; Varnek, A. *J. Comput. Chem.* **1996**, *17*, 864–877.
(63) Cortis, C. M.; Friesner, R. A. *J. Comput. Chem.* **1997**, *18*, 1591–1608.
(64) Purisima, E. O. *J. Comput. Chem.* **1998**, *19*, 1494–1504.
(65) Boschitsch, A. H.; Fenley, M. O.; Zhou, H.-X. *J. Phys. Chem. B* **2002**, *106*, 2741–2754.
(66) Chen, F.; Chipman, D. M. *J. Chem. Phys.* **2003**, *119*, 10289–10297.
(67) Bordner, A. J.; Huber, G. A. *J. Comput. Chem.* **2003**, *24*, 353–367.
(68) Friedman, H. L.; Krishnan, C. V. Thermodynamics of Ionic Hydration. In *Water: A Comprehensive Treatise*; Franks, F., Ed.; Plenum Press: New York, 1973; Vol. 3, pp 1−118.

JP801960P